Rapid Biomolecular Trifluoromethylation Using Cationic Aromatic Sulfonate Esters as Visible Light-Triggered Radical Photocages

Nicholas J. Kuehl[a] and Michael T. Taylor[b*]

[a]University of Wyoming, Department of Chemistry, Laramie, WY 82071

[b]University of Arizona, Department of Chemistry & Biochemistry, Tucson, AZ 85721

ABSTRACT: Described here is a photo-decaging approach to radical trifluoromethylation of biomolecules. This was accomplished by designing a quinolinium sulfonate ester that, upon absorption of visible light, achieves decaging *via* photolysis of the sulfonate ester to ultimately liberate free trifluoromethyl radicals that are trapped by π-nucleophiles in biomolecules. This photo-decaging process enables protein and protein-interaction mapping experiments using trifluoromethyl radicals that require only one second reaction times and low photocage concentrations. In these experiments, aromatic side chains are labelled in an environmentally dependent fashion, with selectivity observed for tryptophan (Trp), followed by histidine (His) and tyrosine (Tyr). Scalable peptide trifluoromethylation through photo-decaging is also demonstrated, where bespoke peptides harboring trifluoromethyl groups at tryptophan residues can be synthesized with five to seven minute reaction times and good yields.

Owing to its biological orthogonality, nuclear spin, and the radioactivity of its isotopes, the incorporation of fluorine and fluorinated functional groups into biomolecular structure has found widespread applications in structural biochemistry and imaging[1]. Moreover, fluorinated functional groups, including the trifluoromethyl group, have become privileged moieties in medicinal chemistry; a result of the combination of hydrophobicity, relatively minimal steric profile, and strong electron-withdrawing properties[2]. Owing to these qualities, the incorporation of trifluoromethyl groups into peptides and

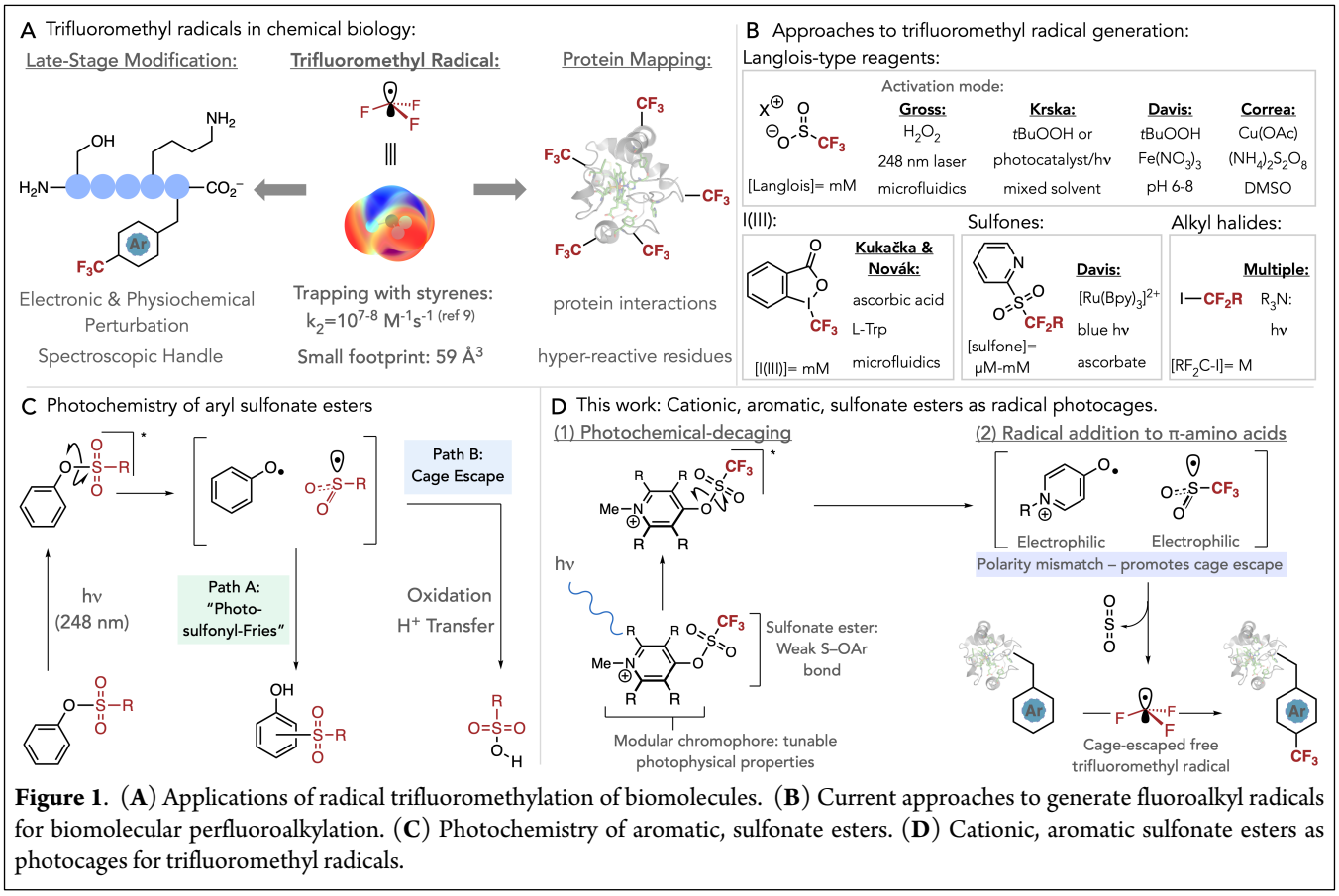

Figure 1. (**A**) Applications of radical trifluoromethylation of biomolecules. (**B**) Current approaches to generate fluoroalkyl radicals for biomolecular perfluoroalkylation. (**C**) Photochemistry of aromatic, sulfonate esters. (**D**) Cationic, aromatic sulfonate esters as photocages for trifluoromethyl radicals.

proteins at specific sites is of interest as it can enable precision alteration of physiochemical properties with minimal steric perturbations[3]. Many elegant approaches have been developed for trifluoromethylation of small molecule organics, yet many of these lack biocompatibility[4]. By comparison, there are relatively few approaches compatible with biomolecular structures, which revolve around electrophilic trifluoromethylation or genetic-engineering[5].

Alternatively, radical-based approaches have been used to achieve biomolecular trifluoromethylation. The use of Langlois's reagent to access trifluoromethyl radicals under either oxidizing or photo-oxidizing conditions[6] has been adapted by Gross[7a], Krska[7b], Davis and Gouverneur[7c,d], and Correa[7e], as well as others[5a], for radical trifluoromethylation in peptides and proteins with wide variations in chemoselectivity. Davis and Gouverneur have also reported similar radical difluoroalkylations of proteins through photocatalyzed activation of sulfonyl pyridines[8a,b]. Recently, hypervalent iodine reagents were shown by Beier[8c] and Kukačka and Novák[8d] to enable radical biomolecular perfluoroalkylation under photochemical[8c] or reducing conditions[8d]. Perfluoroalkyl iodides have also enabled radical fluoroalkylation of protected peptides[5a] *via* a halogen-bonding mechanism[8e]. A particular attraction to protein trifluoromethylation with trifluoromethyl radicals stems from the ultra-rapid kinetics of radical trapping by π-based nucleophiles; with rate constants of 10^{7-8} $M^{-1}s^{-1}$ measured for trapping with styrene derivatives[9]. This voracious electrophilicity, combined with its small size (~59 Å^3), imbue the trifluoromethyl radical with ideal characteristics as a probe for mapping higher-order protein structures[7a] as well as enabling expedient access to fluorinated peptides and proteins.

We propose that a photo-decaging approach in which trifluoromethyl radicals are generated *in situ* through an optically triggered, unimolecular process could enable us to exploit the rapid kinetics of radical addition to π-nucleophiles under mild conditions and with spatiotemporal control. We posited that this could be achieved by using aromatic-sulfonate esters as a photocage for trifluoromethyl radicals. Aromatic sulfonate esters possess a weak S–OAr bond that homolytically cleaves upon photoexcitation to generate a sulfonyl- and aryloxy radical pair that can recombine in a photo-Fries type rearrangement[10]. Alternatively, radical cage escape can occur; liberating free sulfonyl- and phenoxy radicals that lead to the formation of sulfonic acids and other byproducts (Figure 1C). Exploiting this mechanistic regime for the purpose of generating trifluoromethyl radicals could be realized using aryl trifluoromethanesulfonate (triflate) esters that, upon photolysis, generate a sulfonyl radical that desulfonylates to liberate a trifluoromethyl radical[10]. We expanded this hypothesis by proposing that a cationic, aromatic chromophore would encourage photolysis by further weakening the photolabile S–OAr bond whilst also exploiting polar effects[11] to encourage radical cage escape; ultimately leading to the efficient liberation of free trifluoromethyl radicals for trapping with peptides and proteins (Figure 1D). However, it was recognized that this design results in an electron-deficient aryl triflate that may be prone to hydrolysis, and any practical design should ensure good thermal stability in aqueous buffer.

We therefore synthesized photocages **1**-**5** *via* a simple triflation of a pyridone or quinolone precursor with trifluoromethanesulfonic anhydride, followed by assessments of each's absorption properties and hydrolytic stability in phosphate buffer (pH 7.4 in D_2O). While pyridinium triflate **1** possesses little absorption beyond 300 nm and modest stability, the additional conjugation in quinolinium salts **2**-**3** results in a bathochromic shift of absorption to the UVA-optical window. However, these compounds were found to be highly unstable,

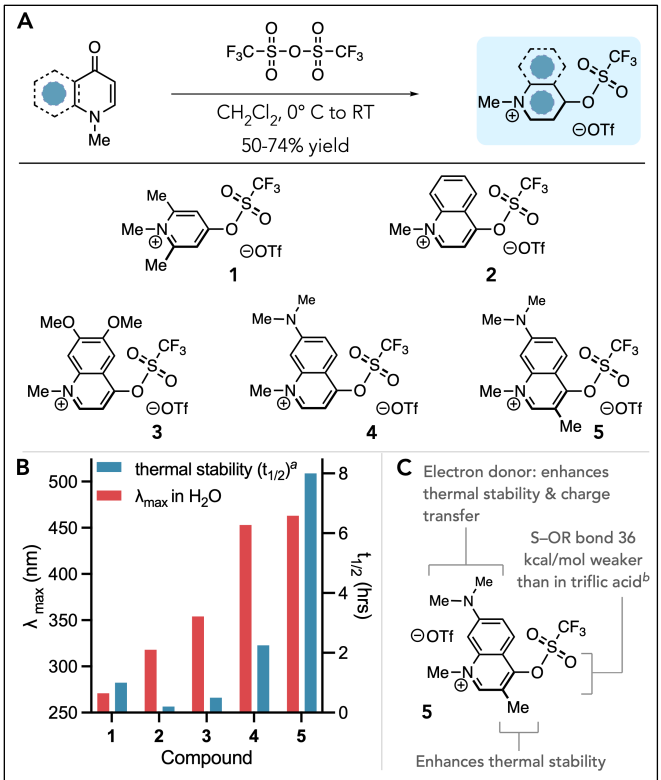

Figure 2. (**A**) Synthesis of photocages **1**-**5**. (**B**) Assessment of thermal stability and absorption properties. (**C**) Key structural properties of **5**. [a]Measured in 20 mM Na_2HPO_4 (pH 7.4) buffered D_2O. [b]Average value from DFT calculations using three different theories.

with $t_{1/2} \leq 0.5$ hrs in both instances (Figure 2B). Installation of a dimethylamino group in the 7-position of the quinolinium scaffold in analog **4** significantly tempered the electrophilicity of the quinolinium-triflate and extended the half-life to 2 hrs whilst also shifting absorbance into the visible spectrum (λ_{max}= 453 nm). Installation of a methyl group in the 3-position in **5** produces a marked enhancement in half-life, with $t_{1/2}$=8 hrs whilst further shifting absorbance to the visible (λ_{max}= 463 nm). DFT calculations suggest the S–OAr bond in **5** is weakened by 36 kcal/mol compared to triflic acid and should therefore be sufficiently weak enough to be cleaved upon photoexcitation whilst TDDFT calculations (CAMB3LYP/6-31+G(d,p) SMD=H_2O level of theory) support a significant charge-transfer component to photoexcitation.

With a stable photocage in hand, we then demonstrated the viability of **5** as a radical photocage by irradiating a solution of model protein lysozyme (10 μM), reactive oxygen species scavenger Tiron (50 μM), and **5** (100 μM) in pH 7.4 phosphate buffer using a Kessil PR-160 456 nm LED in a Hepatochem reactor for one second. Intact MS analysis of the crude reaction mixture indicated up to three trifluoromethyl groups were incorporated into lysozyme with a net 66% conversion of unmodified lysozyme to trifluoromethylated protein. A peptide mapping workflow was performed to identify modification sites and to estimate through semi-quantitation the extent of modification at different residues[7a]. This workflow allowed us to identify three modifications on lysozyme, with W62 being the

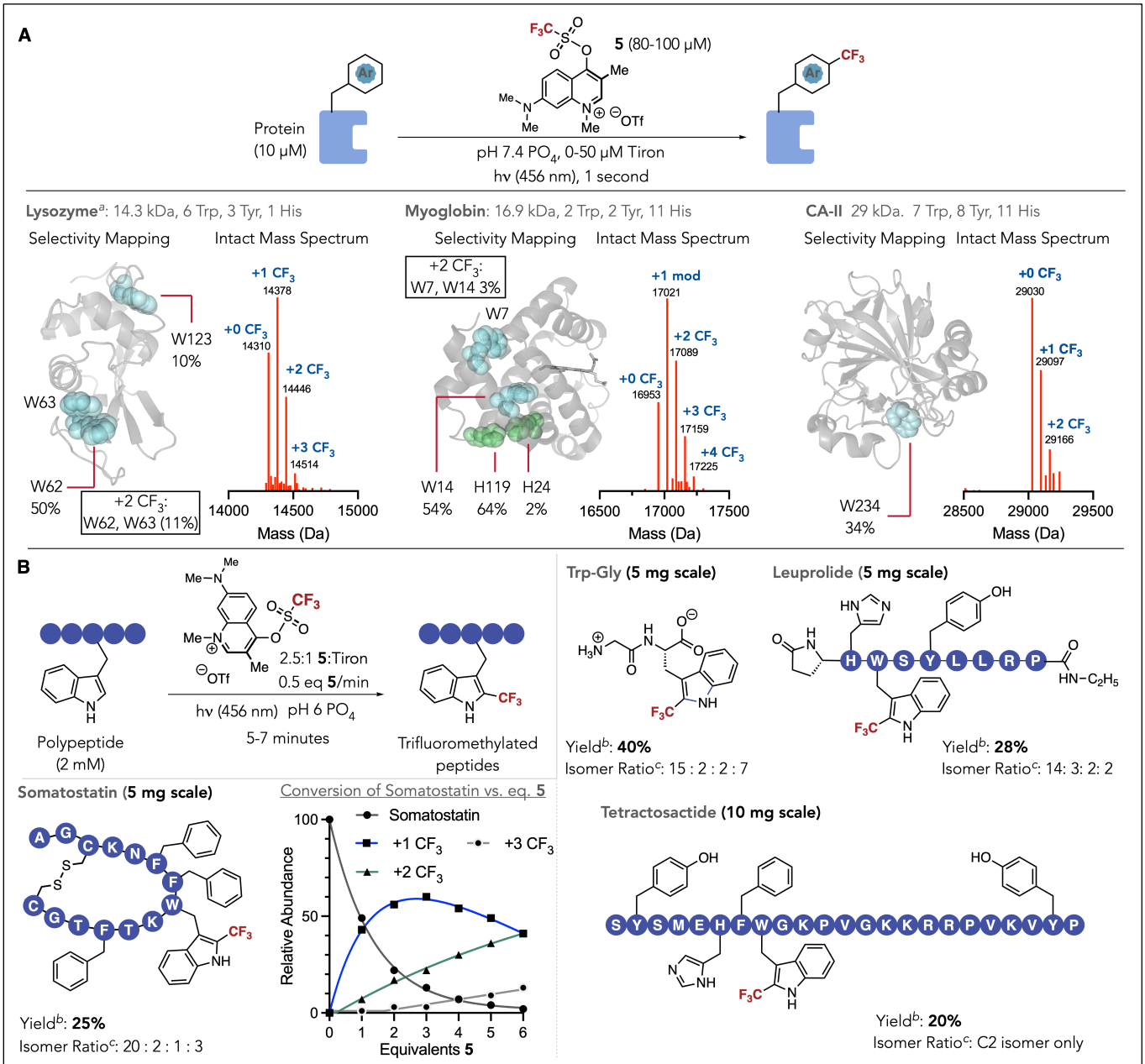

Figure 3. (**A**) Protein labelling and peptide mapping with **5**. (**B**) Preparative scale synthesis of trifluoromethylated peptides with **5**. [a] Intact mass of experiment using 50 μM Tiron, peptide mapping performed using 20 mM Tiron. [b]Isolated yields that are validated by qNMR. [c]Isomer ratios were assigned *via* ^{19}F-NMR and are listed in the following order: C2:C4:C7:+2 CF_3.

primary modification site along with minor modification levels observed on W63 and W123. We next explored labelling of Myoglobin, a 16.9 kDa, heme-containing protein possessing 2 Trp, 2 Tyr, and 11 His residues. Irradiation at 456 nm of myoglobin (10 μM) in the presence of **5** (80μM) for 1 second resulted in the formation of Myoglobin-CF_3 conjugates harboring up to 4 trifluoromethyl groups. Peptide mapping revealed H119 to be the primary site of modification, followed by W14, H24, and W7. H119 participates in H-bonding with H24[12], and this result suggests that this may enhance the nucleophilicity of H119. The context-dependent nature of protein trifluoromethylation was assessed against carbonic anhydrase II (CAII). CAII has 7 Trp, 8 Tyr, and 11 His residues, but most of these are buried within the protein's tertiary structure. Thus, trifluoromethylation of CAII with **5** (100 μM) and Tiron (20 μM) resulted in lower levels of labelling, with only a single modification site at W234 identifiable by peptide mapping. Taken together, these experiments indicated that radical trifluoromethylation with **5** displays chemoselectivity for nucleophilic and electron-rich aromatic residues.

We next sought to develop a procedure for radical trifluoromethylation of aromatic amino acid-containing peptides on a preparative scale using **5**. In order to avoid the pitfalls associated with generating high concentrations of radicals, we developed a process in which a solution containing **5** and tiron (2.5:1 ratio) in 20% CH_3CN:H_2O is added at a rate of 0.5 equivalents **5**/min *via* syringe pump to a buffered, 2 mM solution of peptide substrate that is under constant irradiation with 456 nm light in a Hepatochem reactor. This process was applied to the trifluoromethylation of peptide hormone Somatostatin. Conversion vs. equivalents of **5** added was monitored as shown in the plot in Figure 3B; which revealed that maximal +1 CF_3

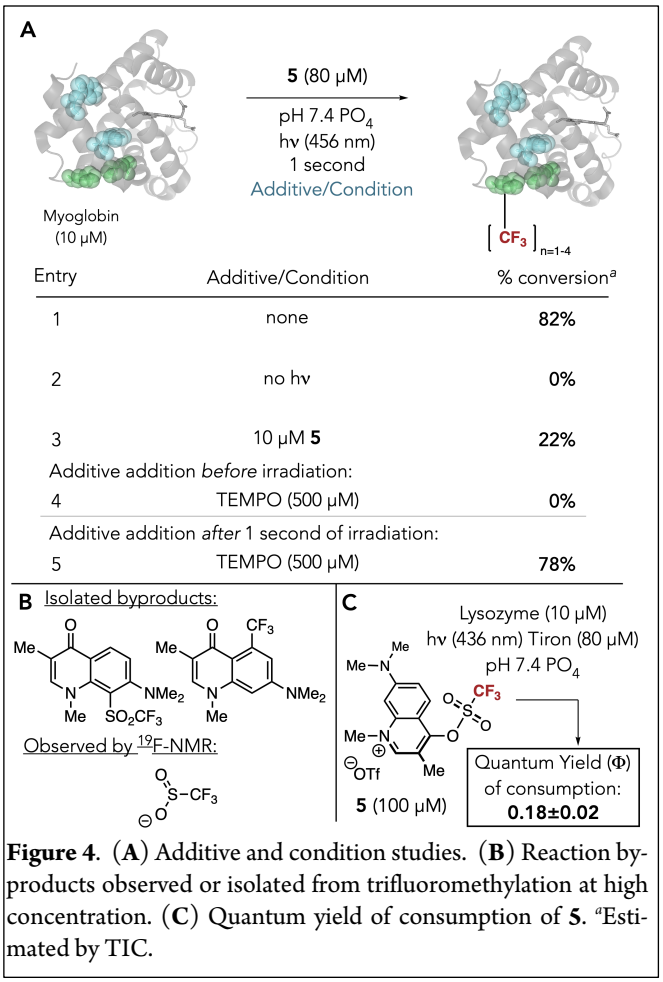

Figure 4. (**A**) Additive and condition studies. (**B**) Reaction byproducts observed or isolated from trifluoromethylation at high concentration. (**C**) Quantum yield of consumption of **5**. [a]Estimated by TIC.

modification occurs after the addition of three equivalents of **5**. Using this information, we performed a 5 mg scale trifluoromethylation reaction of Somatostatin with the addition of three equivalents of **5** over a six-minutes plus one additional minute of irradiation. Somatostatin-CF_3 adducts were then purified by HPLC and resulted in a total of 25% isolated yield of Somatostatin-CF_3 conjugates with trifluoromethylation observed at Trp. We also observed regioisomers of trifluoromethylation products, with the predominant isomer occurring at the indole C2 position of Trp. Minor isomers harboring trifluoromethyl groups at C4 and C7, as well as low levels (<3%) of +2 CF_3 modified Trp were also isolated. Extension of this method to other peptides, including Gly-Trp (0.2 kDa, 1 Trp residue, 5 minute reaction time), Leuprolide (1.2 kDa, 1 His, 1 Tyr, 1 Trp, 7 minute reaction time), and Tetracosactide (2.9 kDa, 2 Tyr, 1 His, 1 Phe, 1 Trp, 7 minute reaction time), smoothly afforded trifluoromethylated conjugates in 20-40% isolated yields; with Trp being the primary site of modification in all instances.

Next, we sought to validate mechanistic aspects of trifluoromethylation with **5**. We propose that trifluoromethylation is achieved *via* two mechanistic manifolds as shown in Figure 1D and includes: (1) optically-triggered photolysis of a labile S–OAr bond to form a quinoloxy-sulfonyl radical pair and (2) following cage escape, thermal extrusion of SO_2 and radical alkylation of π-nucleophiles with free trifluoromethyl radicals. Evidence supporting a free radical labelling mechanism includes: (1) the observation of regioisomers of trifluoromethylated Trp-conjugates in Figure 3B[6b,c,7b-d] (2) the inhibition of trifluoromethylation of myoglobin with **5** when the reaction is co-incubated with TEMPO[9] (Figure 4A, entry 4) and (3) by observing trifluoromethanesulfinate anion by ^{19}F-NMR and isolating sulfonylated and trifluoromethylated quinolone adducts from a high-concentration photo-decaging reaction of **5** (3 mM) with Gly-Trp (1 mM) in buffered D_2O:CD_3CN (Figure 4B). One-second reaction times for protein labelling were validated through a trapping experiment wherein TEMPO (500 μM) that was added to the reaction at 1 second of irradiation did not significantly perturb reaction conversion (Figure 4A, entry 5). The vigorous reactivity of **5** was further validated through a 1:1 stoichiometry reaction between Myoglobin (10 μM) and **5** (10 μM), which produced a significant 22% conversion with a 1 second irradiation time (Figure 4A, entry 3). Finally, the requirement for optical triggering was validated by incubation of Myoglobin with **5** in the absence of light (Figure 4A, entry 2) and quantified by estimating a quantum yield of $\Phi_{conversion}$ =0.18±0.02 for the consumption of **5** during lysozyme labelling (Figure 4C).

Using **5** as a photocage offers a mild and mechanistically distinct approach to protein labelling with electrophilic radicals. We therefore posited that **5** may be useful in peptide mapping experiments of protein-ligand and protein-protein interactions, wherein labelling outcomes correlate to changes biomolecular environments[13] (Figure 5A). Based upon our observation of labelling of Trp-62 in lysozyme's active site, we opted to establish a proof-of-concept by mapping the binding interaction between lysozyme and tri-saccharide NAG3; an interaction that was elegantly mapped by Vachet using high concentrations of Trp-selective bioconjugation reagent HNSB[14]. Thus, increasing concentrations of NAG3 ligand were titrated into a solution of 10 μM lysozyme, 100 μM **5**, and 50 μM Tiron, followed by irradiation with 456 nm light for 1 second (Figure 5B). Plotting the change in labelling conversion vs. NAG3 concentration enabled the estimation of the binding affinity of NAG3 to lysozyme (k_d= 35.9 μM).

Finally, we investigated the mapping of protein-peptide interactions in a representative system. We selected the calmodulin-myosin light chain kinase interaction to provide a platform to assess this possibility and to explore complementarity with current approaches[13,15]. We took both bovine Calmodulin and the peptide sequence of the myosin light chain that actively binds to Calmodulin (M13 peptide). The M13 peptide sequence features a single Trp (W4) and two Phe residues. Binding of M13 to calmodulin results in a ternary structure of the two biomolecules in which the M13-W4 residue is buried and should be shielded from CF_3 radicals[16]. Bovine calmodulin features three Tyr and His residues: Y100, Y139 and H108. Each peptide was individually treated with **5** (100 μM), Tiron (20 μM), and $CaCl_2$ (100 μM) in pH 7.4 PBS and one second of irradiation with 456 nm light (Figure 5C). Trifluoromethylation of M13 peptide under these conditions led to robust labelling exclusively at W4, whilst labelling of unbound calmodulin yielded low levels of modification on Y100 and Y139. M13 and calmodulin were then complexed in 1:1 stoichiometry, followed by trifluoromethylation under identical conditions. Intact MS analysis and peptide mapping indicated a dramatic loss of W4-trifluoromethylation whilst calmodulin modification remained similar (Figure 5C, inset). Taken together, protein mapping with **5** enables the facile exploration of changes in environments to aromatic amino acid residues; wherein the ability to use low concentrations of proteins and **5**, as well as short reaction times, minimize the risk of non-specific interactions obfuscating results. Aromatic residues have a wide range of functions in proteins and protein interactions, and the ability to probe for context-dependent reactivity is

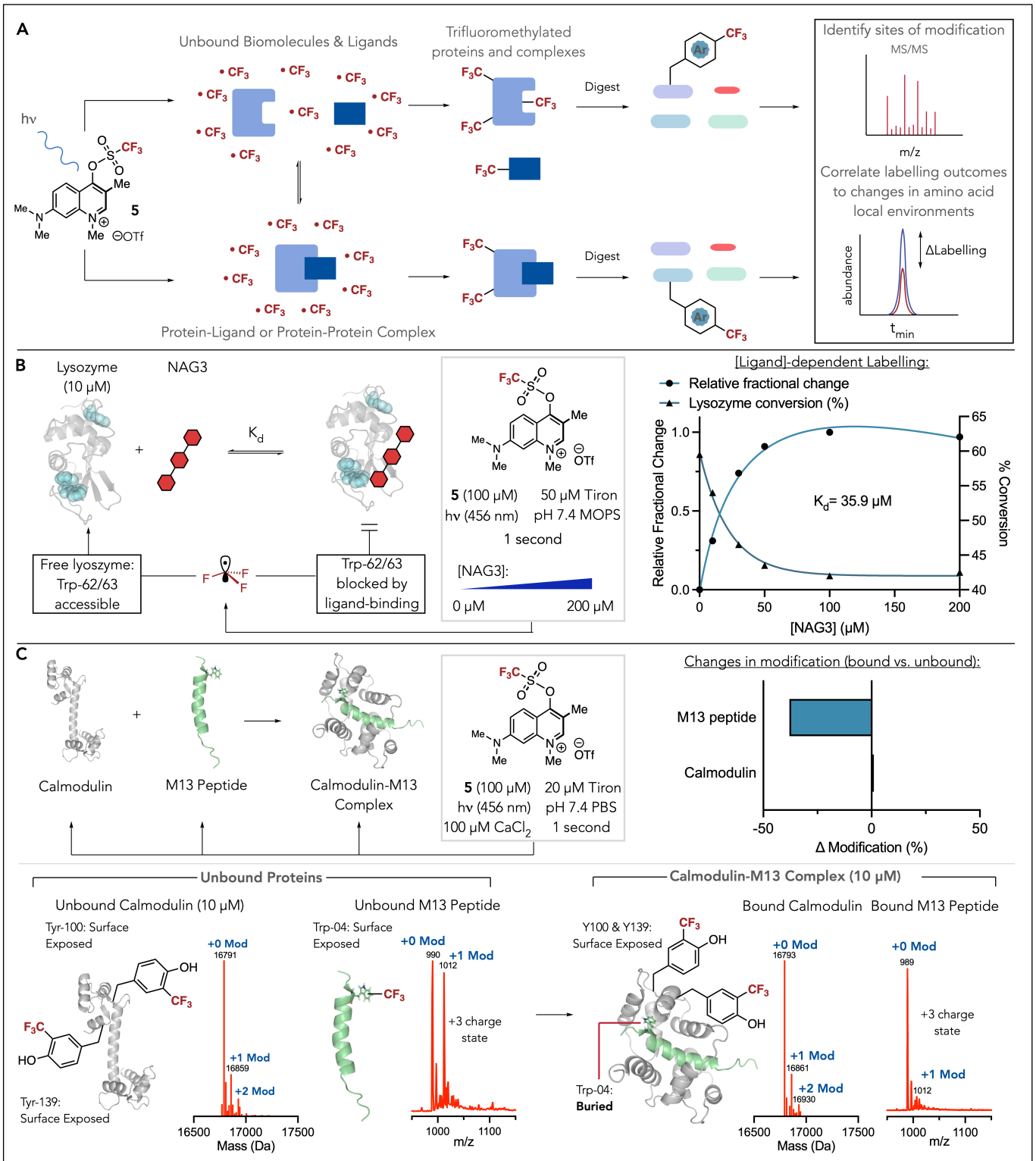

Figure 5. (**A**) A photo-decaging approach to protein interaction mapping with **5**. (**B**) Mapping of the interaction of lysozyme with NAG3 using radical trifluoromethylation with **5**. (**C**) Mapping of the calmodulin-M13 complex using **5**.

an increasingly appreciated approach for revealing amino acid function and new sites for drug design[17].

In summary, we have developed cationic, quinolinium scaffold **5** as a photocage that enables trifluoromethyl radical release through optical triggering with visible light. Mechanistic analyses indicate that **5** enables ultra-rapid protein labelling *via* a photolysis of a labile S–O bond followed by liberation of a free trifluoromethyl radical. We show that **5** is adaptable toward multiple workflows, including protein and protein-interaction mapping, as well as for preparative scale trifluoromethylation of peptides.

ASSOCIATED CONTENT

Supporting information includes experimental procedures for photocage synthesis, protein trifluoromethylation, preparative scale peptide trifluoromethylation, mechanistic studies, computational analysis, and small molecule characterization.

The Supporting Information is available free of charge on the ACS Publications website.

AUTHOR INFORMATION

Corresponding Author

* mtaylor6@arizona.edu

ORCID

Michael T. Taylor: 0000-0002-7655-7222

Nicholas J. Kuehl: 0000-0003-3640-8596

Notes

No competing financial interests have been declared.

Funding Sources

No competing financial interests have been declared.

ACKNOWLEDGMENT

We thank the National Institute of General Medical Sciences (R35 GM143120) for financial support.

REFERENCES

(1) (a) Danielson, M.A.; Falke, J.J. Use of ^{19}F-NMR to Probe Protein Structure and Conformational Changes. *Annu. Rev. Biophys. Biomol. Struct.* **1996**, 25, 163-195. (b) Tirotta, I.; Dichiarante, V.; Pigiacelli, C.; Cavallo, G.; Terraneo, G.; Bombelli, F.B.; Metrangolo, R.; Resnati, G. ^{19}F- Magnetic Resonance, Imaging (MRI): From Design of Materials to Clinical Applications. *Chem. Rev.* **2015**, 115, 1106-1129. (c) Arnston, K.E.; Pomerantz, W.C.K. Protein-Observed Fluorine NMR: A bioorthogonal Approach for Small Molecule Discovery. *J. Med. Chem.* **2016**, 59, 5158-5171. (d) Lee, S.; Xie, J.; Chen, X. Peptide-Based Probes for Targeted Molecular Imaging. *Biochemistry*, **2010**, 49, 1364-1376. (e) Vallabhajosula, S. ^{18}F-Labeled Positron Emission Tomographic Radiopharmaceuticals in Oncology: An Overview of Radiochemistry and Mechanisms of Tumor Localization. *Semin. Nucl. Med.* **2007**, 37, 400-419. (f) Fani, M.; Maecke, H.R. Radiopharmaceutical development of radiolabelled peptides. *Eur. J. Nucl. Med. Mol. Imaging.* **2012**, 39, S11-S30.

(2) (a) Yale, H.L. The Trifluoromethyl Group in Medicinal Chemistry. *J. Med. Chem.* **1959**, 1, 121-133. (b) Monkovic, J.M.; Gibson, H.; Sun, J.W.; Montclare, J.K. Fluorinated Protein and Peptide materials for Biomedical Applications. *Pharmaceuticals*, **2022**, 15, 1201-1237. (c) Hagmann, W.K. The Many Roles for Fluorine in Medicinal Chemistry. *J. Med. Chem.* **2008**, 51, 4359-4369. (d) Zhou, Y.; Wang, J.; Gu, Z.; Wang, S.; Zhu, W.; Aceña J. L.; Soloshonok, V. A.; Izawa, K.; Liu, H. Next Generation of Fluorine-Containing Pharmaceuticals, Compounds Currently in Phase II-II Clinical Trials of Major Pharmaceutical Companies: New Structural Trends and Therapeutic Areas. *Chem. Rev.*, **2016**, 116, 422-518.

(3) (a) Marsh, E.N.G. Fluorinated Proteins: From Design and Synthesis to Structure and Stability. *Acc. Chem. Res.* **2014**, 47, 2878-2886. (b) Abula, A.; Xu, Z.; Zhu, Z.; Peng, C.; Chen. Z.; Zhu, W.; Aisa, H.A. Substitution Effect of the Trifluoromethyl Group on the Bioactivity in medicinal Chemistry: Statistical Analysis and Energy Calculation. *J. Chem. Inf. Model.* **2020**, 60, 6242-6250. (c) Miller, M.A.; Sletten, E.M. Perfluorocarbons in Chemical Biology. *ChemBioChem*. **2020**, 21, 3451-3462.

(4) (a) Studer, A. A "Renaissance" in Radical Trifluoromethylation. *Angew. Chem. Int. Ed.,* **2012,** 51, 8950-8958. (b) Charpentier, J.; Früh, N.; Togni, A. Electrophilic Trifluoromethylation by Use of Hypervalent Iodine Reagents. *Chem. Rev.* **2015**, 115, 650-682. (c) Barata-Vallejo, S.; Lantaño, B.; Postigo, A. Electrophilic Trifluoromethylating Reagents. *Chem. Eur. J.* **2014**, 20, 16806-16829. (d) Mandal, D.; Maji, S.; Pal, T.; Sinha, S.K.; Maiti, D. Recent advances in transition metal-mediated trifluoromethylation reactions. *Chem. Commun.* **2022**, 58, 10442-10468. (e) Tomashenko, O.A.; Grushin, V.V. Aromatic Trifluoromethylation with metal Complexes. *Chem. Rev.* **2011**, 111, 4475-4521. (f) Liu, X.; Xu, C.; Wang, M.; Liu, Q. Trifluoromethyltrimethylsilane: Nucleophilic Trifluoromethylation and Beyond. *Chem. Rev.* **2015**, 115, 683-730. (g) Furuya, T.; Kamlet, A.S.; Ritter, T. Catalysis for fluorination and trifluoromethylation. *Nature.* **2011**, 473, 470-477. (h) Alonso, C.; de Marigorta, E.M.; Rubiales, G.; Palacios, F. Carbon Trifluoromethylation Reactions of Hydrocarbon Derivatives and Heteroarenes. *Chem. Rev.* **2015**, 115, 1847-1935.

(5) For a recent review on trifluoromethylation of peptides: (a) Guerrero, I.; Correa, A. Site-Selective Trifluoromethylation Reactions of Oligopeptides. *Asian J. Org. Chem.* **2020**, 9, 898-909.

For genetic-code expansion approaches: (b) Wang, Y-S.; Fang, X.; Chen, H-Y.; Wu, B.; Wang, Z.U.; Hilty, C.; Liu. W.R. Genetic Incorporation of Twelve *meta*-Substituted Phenylalanine Derivatives Using a Single Pyrrolysyl-tRNA Synthetase Mutant. *ACS. Chem. Biol.* **2013**, 8, 405-415. (c) Mehl, R.A.; Jackson, J.C. Site-Specific Incorporation of a ^{19}F-Amino Acid into Proteins as an NMR Probe for Characterizing Protein Structure and Reactivity. *J. Am. Chem. Soc.* **2007**, 129, 1160-1166.

(6) (a) Langlois, B. R.; Laurent, E., Roidot, N. Trifluoromethylation of Aromatic Compounds with Sodium Trifluoromethanesulfinate under oxidative conditions. *Tetrahedron Letters.* **1991**, 32, 51, 7525-7528. (b) Fujiwara, Y.; Dixon, J. A.; O'Hara, F.; Funder, E. D.; Dixon, D. D.; Rodriguez, R. A.; Baxter, R. D.; Herle, B.; Sach, N.; Collins, M. R.; Ishihara, Y.; Baran, P. S. Practical and innate C-H functionalization of heterocycles. *Nature.* **2012,** 492(7427), 95-99. (c) Nagib, D. A.; MacMillan, D. W. C. Trifluoromethylation of arenes and heteroarenes by means of photoredox catalysis. *Nature.* **2011,** 480, 224-228.

(7) (a) Cheng, M.; Zhang, B.; Cui, W.; Gross, M.L. Laser-Initiated Radical Trifluoromethylation of peptides and Proteins: Application to Mass-Spectrometry-Based Protein Footprinting. *Angew. Chem. Int. Ed.* **2017**, 56, 14007-14010. (b) Ichiishi, N.; Caldwell, J. P.; Lin, M.; Zhong, W.; Zhu, X.; Streckfuss, E.; Kim, H.; Parish, C. A.; Krska, S. W. Protecting group free radical C-H trifluoromethylation of peptides. *Chem. Sci.* **2018,** 9, 4168-4175. (c) Imiołek, M.; Karunanithy, G.; Ng, W.; Baldwin, A. J.; Gouverneur, V.; Davis, B. G. Selective Radical Trifluoromethylation of Native Residues in Proteins. *J. Am. Chem. Soc.* **2018,** 140, 1568-1571. (d) Kee, C.W.; Tack, O.; Guibbal, F.; Wilson, T.C.; Isenegger, P.G; Imiołek, M.; Verhoog, S.; Tilby, M.; Boscutti, G.; Ashworth, S.; Chupin, J.; Kashani, R.; Poh, A.W.J.; Sosabowski, J.K.; Macholl, S.; Plisson, C.; Cornelissen, B.; Willis, M.C.; Passchier, J.; Davis, B.G.; Gouverneur, V. ^{18}F-Trifluoromethanesulfinate Enables Direct C-H ^{18}F-Trifluoromethylation of Native Aromatic Residues in Peptides. *J. Am. Chem. Soc.* **2020**, 142, 1180-1185. (e) Guerrero, I.; Correa, A.; *Org. Lett.* **2020**, 5, 1754-1759.

(8) (a) Josephson, B.; Fehl, C.; Isenegger, P.G.; Nadal, S.; Wright, T.H.; Poh, A.W.J.; Bower, B.J.; Giltrap, A.M.; Chen, L.; Batchelor-McAuley, C.; Roper, G.; Arisa, O.; Sap, J.B.I.; Kawamura, A.; Baldwin, A.J.; Mohammed, S.; Compton, R.G.; Gouverneur, V.; Davis, B.G. Light-driven post-translational installation of reactive protein side chains. *Nature.* **2020**, 585, 530-537. (b) Imiołek, M.; Isenegger, P.G.; Ng, W-L.; Khan, A.; Davis, B.G. Residue-Selective Protein C-Formylation via Sequential Difluoroalkylation-Hydrolysis. *ACS. Cent. Sci.* **2021**, 7, 145-155. (c) Rahimidashaghoul, K.; Klimánková, I.; Hubálek, M.; Matousek, V.; Filgas, J.; Slavícek, P.; Slanina, T.; Beier, P. Visible-Light-Driven Fluoroalkylation of Tryptophan Residues in Peptides. *ChemPhotoChem*. **2021**, 5, 43–50. (d) Fojtík, L.; Fiala, J.; Pompach, P.; Chmelík, J.; Matousek, V.; Beier, P.; Kukacka, Z.; Novák, P. *J. Am. Chem. Soc.* **2021**, 143, 20670–20679. (e) Wang, Y.; Wang, J.; Li, G-X.; Chen, G. Halogen-Bond-Promoted Photoactivation of Perfluoroalkyl Iodides: A Photochemical Protocol for Perfluoroalkylation Reactions. *Org. Lett.* **2017**, 19, 1442-1445.

(9) Hartmann, M.; Li, Y.; Studer, A. Determination of rate constants for trifluoromethyl radical addition to various alkenes *via* a practical method. *Org. Biomol. Chem.* **2016**, 14, 206-210.

(10) (a) Stratenus, J.L.; Havinga, E. Photoreactions of Aromatic Compounds IX. *Rec. Trav. Chim.* **1966**, 85, 434-436. (b) Andraos, J.; Barclay,

G.G.; Medeiros, D.R.; Baldovi, M.V.; Scaiano, J.C.; Sinta, R. Model Studies on the Photochemistry of Phenolic Sulfonate Photoacid Generators. *Chem. Mater.* **1998**, 10, 1694-1699. (c) Kageyama, Y.; Ohshima, R.; Sakurama, K.; Fujiwara, Y.; Tanimoto, Y.; Yamada, Y.; Aoki, S. Photochemical Cleavage Reactions of 8-Quinolinyl Sulfonates in Aqueous Solution. *Chem. Pharm. Bull.* **2009**, 57, 1257-1266. (d) Zeppuhar, A.N.; Wolf, S.M.; Falvey, D.E. *J. Phys. Chem. A.* **2021**, 125, 5227-5236.

(11) (a) Walling, C. *Free Radicals in Solution*, John Wiley & Sons, Inc. New York, 1957. (b) Fisher, H.; Radom, L. Factors Controlling the Addition of Carbon-Centered Radicals Alkenes-An Experimental and Theoretical Perspective. *Angew. Chem. Int. Ed.* **2001**, 40, 1340-1371.

(12) Chu, K.; Vojtechovský, J.; McMahon, B.H.; Sweet, R.M.; Brendzen, J.; Schlichting. Structure of a ligand-binding intermediate in wild-type carbonmonoxy myoglobin. *Nature*. **2000**, 403, 921-923.

(13) Liu, X.R.; Zhang, M.M.; Gross, M.L. Mass Spectrometry-Based Protein Footprinting for Higher-Order Structure Analysis: Fundamentals and Applications. *Chem. Rev.* **2020**, 120, 4355-4454.

(14) Liu, T.; Marcinko, T.M.; Vachet, R.W. Protein-Ligand Affinity Determinations Using Covalent Labeling-Mass Spectrometry. *J. Am. Mass. Spectrom.* **2020**, 31, 1544-1553.

(15) Zhang, H.; Gau, B.C.; Jones, L.M.; Vidavsky, I.; Gross, M.L. Fast Photochemical Oxidation of Proteins for Comparing Structures of Protein-Ligand Complexes: The Calmodulin-Peptide Model System. *Anal. Chem.* **2011**, 83, 311-318.

(16) Ikura, M.; Clore, C.M.; Gronenborn, G.Z.; Klee, C.B.; Bax, A. Solution Structure of a Calmodulin-Target Peptide Complex by Multidimensional NMR. *Science*. **1992**, 256, 632-638.

(17) (a) Ma, B.; Nussinov, R. Trp/Met/Phe Hot Spots in Protein-Protein Interactions: Potential Targets in Drug Discovery. *Curr. Top. Med. Chem.* **2007**, 7, 999-1005. (b) Liao, S-M.; Du, Q-D.; Meng, J-Z.; Pang, Z-W.; Huang, R-B. The multiple roles of histidine in protein interactions. *Chem. Cent. J.* **2013**, 7, article number 44. (c) Spradlin, J.N.; Zhang, E.; Nomura, D.K. Reimagining Druggability Using Chemoproteomic Platforms. *Acc. Chem. Res.* **2021**, 54, 1801-1813.

Insert Table of Contents artwork here